Journal of Applied Polymer Science

Electrospinning Polycaprolactone Dissolved in Glacial Acetic Acid: Fiber Production, Nonwoven Characterization, and *In Vitro* Evaluation

José Luís Ferreira,[1] Susana Gomes,[1] Célia Henriques,[1] João Paulo Borges,[2] Jorge Carvalho Silva[1]

[1]Departamento de Física, Faculdade de Ciências e Tecnologia, Centro de Física e Investigação Tecnológica, CeFITec, Universidade Nova de Lisboa, 2829-516, Caparica, Portugal

[2]Departamento de Ciência dos Materiais, Faculdade de Ciências e Tecnologia, Centro de Investigação de Materiais, CENIMAT/I3N, Universidade Nova de Lisboa, 2829-516, Caparica, Portugal

Correspondence to: J. C. Silva (E-mail: jcs@fct.unl.pt)

ABSTRACT: The electrospinning of polycaprolactone (PCL) dissolved in glacial acetic acid and the characterization of the resultant nonwoven fiber mats is reported in this work. For comparison purposes, PCL fiber mats were also obtained by electrospinning the polymer dissolved in chloroform. Given the processing parameters chosen, results show that 14 and 17 wt % PCL solutions are not viscous enough and yield beaded fibers, 20 and 23 wt % solutions give rise to high quality fibers and 26 wt % solutions yield mostly irregular and fused fibers. The nonwoven mats are highly porous, retain the high tensile strain of PCL, and the fibers are semicrystalline. Cells adhere and proliferate equally well on all mats, irrespective of the solvent used in their production. In conclusion, mats obtained by electrospinning PCL dissolved in acetic acid are also a good option to consider when producing scaffolds for tissue engineering. Moreover, acetic acid is miscible with polar solvents, which may allow easier blending of PCL with hydrophilic polymers and therefore achieve the production of electrospun nanofibers with improved properties. © 2014 Wiley Periodicals, Inc. J. Appl. Polym. Sci. **2014**, *131*, 41068.

KEYWORDS: biomaterials; biomedical applications; electrospinning; fibers; mechanical properties

Received 17 March 2014; accepted 27 May 2014
DOI: 10.1002/app.41068

INTRODUCTION

Biodegradable and biocompatible polymers are processed using many different techniques into porous scaffolds that support the growth, differentiation, and migration of cells. These scaffolds are a typical first step in the engineering approach to the production of biological substitutes used to repair tissues or organs in patients having theirs with compromised structure or function.[1–4]

Polycaprolactone (PCL) is a linear aliphatic polyester whose biocompatibility, low melting point, high plasticity, and ductility make it appealing for the production of scaffolds for tissue engineering.[5–11] One of its drawbacks is its hydrophobicity that makes it insoluble in aqueous solvents. Typical good solvents used to dissolve PCL include chloroform,[12–16] acetone,[17–20] methylene chloride,[21,22] hexafluoropropanol,[23] and mixtures thereof.[24] Attempts to electrospin PCL dissolved in glacial acetic acid yielded beaded fibers that became defect free when a salt (pyridine) was added to the solution[25] or when a cosolvent (formic acid) was used.[26] Recently, electrospinning of PCL dissolved in both glacial and 90% acetic acid has been reported.[27] Acetic acid is a moderately good solvent for PCL, although usually not considered as such,[28] and can be removed from the fibers without leaving potentially harmful residues. Several mixtures of good solvents with poor or nonsolvents have also been used with success[10,18,29–32] with the mixture chloroform : methanol in the ratio 3 : 1 being particularly popular.[33–36]

PCL is not the ideal polymer for a tissue engineering scaffold because of lack of cell adhesion sites. Fibroblasts cultured on untreated PCL films or fibers show weak adhesion or rounded morphology, respectively.[34] However, when PCL fibers were postprocessed by alkaline hydrolysis[34] or by air plasma treatment[9] to decrease the average molecular mass of the polymer, thereby increasing the number of terminal OH groups and the hydrophilicity of the membranes, the water contact angle decreased from 120° to 0° and the cells adopted a spread morphology with enhanced adhesion. Moreover, PCL can be blended with other synthetic or natural polymers to reach a synergistic mix of their respective characteristics and impart good mechanical properties and slow degradation rate to the scaffolds produced from blends containing PCL.[11,37–39]

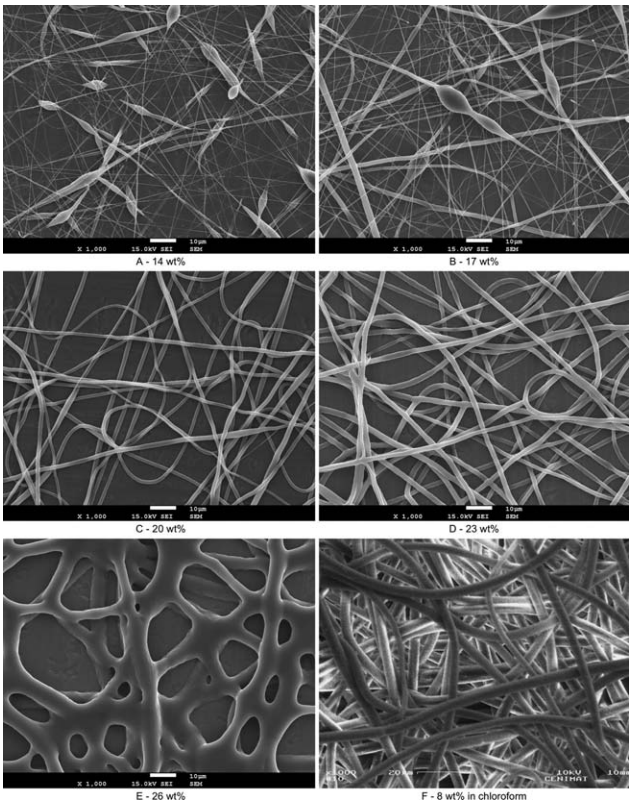

Figure 1. Effect of PCL concentration on fibers morphology of PCL dissolved in acetic acid (A–E); and PCL dissolved in chloroform (F).

Electrospinning is a technique that allows the production of polymeric micro- and nanofibrous scaffolds from precursors that may be polymer solutions, blends or melts.[40–46] During the electrospinning process itself, as the charged polymer jet travels from the needle tip to the collector, the solvent evaporates leading to a gradual decrease of the jet diameter and an increase of local viscosity. After traveling for a short distance, the repulsion between charges transported by the polymer jet causes it to enter a chaotic motion during which the jet bends and whips, causing a further and severe stretching of the jet. Under favorable conditions, upon arrival at the target, the fibers have reached diameters in the nanometer range and are collected as nonwoven fiber mats. Advances in the electrospinning technique allow the production of more complex structures. Examples include the use of multiple spinnerets and collector geometries and arrangements to fabricate a multitude of nanofiber assemblies,[47] the use of coaxial spinnerets to produce core-sheath bicomponent or hollow nanofibers,[48] the encapsulation of drugs,[49,50] micro- and nanoparticles[51] or even cells.[52]

The present study investigated the potential advantages of electrospinning PCL dissolved in acetic acid regarding the morphology of the fibers, the properties of fiber mats and their capability as cell culture substrate. The influence of polymer concentration and feed rate on the morphology and diameter of the fibers was studied. The porosity, mechanical properties, degree of crystallinity, and crystallite size of nonwoven fiber mats obtained under our standard spinning conditions and cell adhesion and proliferation were evaluated and compared to those of fiber mats obtained using a solution of PCL dissolved in chloroform, one of the best and most used solvents of PCL.

EXPERIMENTAL

Materials and Solutions

PCL ($M_n = 80$ kg mol^{-1}) was acquired from Sigma-Aldrich (St. Louis, USA), acetic acid (purity 99.8%) was acquired from Pronolab (Lisboa, Portugal) and chloroform (purity 99%) was acquired from Carlo Erba (Milano, Italy). All materials were used as received.

The PCL pellets were dissolved in glacial acetic acid to produce solutions of concentrations ranging from 14 to 26 wt % and in chloroform to produce an 8 wt % solution. The solutions were mixed with a magnetic stirrer overnight and those with acetic acid were placed in an ultra-sound bath for 30 min to promote a complete dissolution of the polymer.

The polymeric solutions were characterized regarding their surface tension, γ, electrical conductivity, σ, and shear viscosity, η. Surface tension was measured using the pendant drop method in a tensiometer (model CAM101) from KSV (Helsinki, Finland). Electrical conductivity was measured using a conductivity meter (model HI 4521) from Hanna Instruments (Woonsocket, Rhode Island, USA). Shear viscosity was measured using a rotational rheometer (model Bohlin Gemini HR nano) from Malvern Instruments (Worcestershire, UK) equipped with 40 mm cone and plate fixtures.

Fiber Production

The electrospinning apparatus was set up horizontally and employed a static collector (a 20 × 20 cm^2 aluminum plate) covered by an aluminum foil. A syringe pump (New Era Pump Systems, USA) was used to control the polymer solution flow rate and a high voltage DC power supply (Iseg High Voltage, Germany) was used to charge the solution and create the electric field between the needle and the collector. The standard parameters used to electrospin PCL dissolved in acetic acid were: high voltage, 6.0 kV; needle-collector distance, 10.0 cm; feed rate, 0.3 mL h^{-1}; needle, 22 G. The effect of varying the feed rate from 0.3 mL h^{-1} up to 1.3 mL h^{-1} on the resultant fiber diameter was studied. In the case of PCL dissolved in chloroform, the spinning conditions were: high voltage, 13.0 kV; needle-collector distance, 28 cm; feed rate, 0.6 mL h^{-1}; needle, 23G.

Fiber Characterization

The morphology of the electrospun nanofibers was observed using a JEOL 7001 Field Emission Gun Scanning Electron Microscope with the exception of Figure 1(F), which was obtained with a Zeiss DSM 962. All samples were sputter-coated with gold before SEM observation. The fiber diameter was measured by image analysis using ImageJ software (National Institutes of Health, USA).

The porosity, P, of the PCL fiber mats was evaluated from the measured apparent density using the following definition:

$$P = 1 - \frac{\rho_{\text{apparent}}}{\rho_{\text{PCL}}}$$

where ρ_{PCL} is the density of PCL ($\rho_{\text{PCL}} = 1.145$ g cm^{-3} as indicated by the supplier) and ρ_{apparent} is the apparent density of

Table I. Properties of the PCL Solutions Used

Solvent	PCL concentration (wt %)	Surface tension γ/(mN m^{-1})	Conductivity σ/(μS cm^{-1})	Zero shear viscosity η/(Pa s)
Acetic acid	14	28.5	0.039	4.4
	17	28.6	0.029	8.5
	20	30.9	0.026	21
	23	29.7	0.026	42
	26	32.8	0.017	81
Chloroform	8	29.2	0.004	2.21

the fiber mats, calculated from the mass to volume ratio of 5 samples with a 1 cm^2 surface area.

Mechanical properties of as-spun fiber mats obtained with four different feed rates were measured with a uniaxial tensile testing machine from Rheometric Scientific equipped with a 20 N load cell. Twenty specimens were tested for each feed rate at a speed of 5 mm/min. Rectangular samples were cut with a surface area of 10 × 30 mm^2 and mounted on the testing machine such that the pulled length was 10 mm. Thickness of the samples was measured with a digital micrometer (Mitutoyo corporation, Japan).

Structural characterization of PCL fibers was performed by X-ray diffraction (XRD) using CuKα radiation in the range $15° < 2\theta < 35°$ with a PANalytical X'Pert PRO X-ray diffractometer. The diffractograms were fitted with a sum of Voigt functions using the software Igor Pro (Wavemetrics, Portland, USA). A constant background was assumed and included in the fit.

The degree of crystallinity, $w_{c,x}$, was calculated as:

$$w_{c,x} = \frac{I_c}{I_c + I_a}$$

where I_c is the sum of the areas under the peaks resulting from diffraction by the crystalline fraction of the fibers and I_a is the area of the peak resulting from amorphous reflections.[53]

The crystallite size, τ, was calculated from XRD patterns using the Scherrer equation[54]:

$$\tau = \frac{0.89\lambda}{\beta cos\theta}$$

where $\lambda = 0.154$ nm is the wavelength of CuKα radiation, β is the full width at half maximum of the diffraction peak and θ is the diffraction angle.

Experimental values for average fiber diameter, apparent density, fiber mat porosity, and Young's modulus are presented as (mean ± experimental standard deviation). The degree of crystallinity values are presented as (value ± standard combined uncertainty). Statistical significance of the differences between results was evaluated using Student's *t*-test.

Cell Seeding and Culture

Cell culture was carried out with Vero cells (African green monkey kidney epithelial cells). 10^4 cells were seeded on each circular membrane sample with a 0.5 cm^2 area inserted in a cylindrical cup. Cell control culture was performed by plating 4×10^4 cells per well in a 24 well plate (Sarstedt, Germany). Before cell seeding, all scaffolds were sterilized in ethanol 70% (v/v), washed with a phosphate buffered saline solution (PBS) and soaked with complete culture medium 15 min before seeding. Culture medium used was Dulbecco's modified Eagle medium (DMEM) with GlutaMAX^{TM} supplemented with fetal bovine serum (10% v/v), penicillin G (100 units/mL), and streptomycin (100 μg/mL), all from Invitrogen. Cells were maintained in a 5% CO_2 humidified atmosphere at 37°C in a MCO-19AIC(UV) incubator (Sanyo, Japan).

Cell Viability and Morphology

Adhesion and proliferation of cells on the sample membranes and control wells were assessed using the resazurin assay. The adhesion test was performed 20 h after cell seeding and the proliferation tests were performed daily on subsequent days up to the fourth day of culture. To perform the assays, cells were incubated for 3 h in fresh medium supplemented with 10% resazurin (Alfa Aesar, USA) dissolved in PBS at a concentration of 2.5 mg mL^{-1}. Viable cells reduce resazurin, yielding resorufin, whose absorption spectrum is shifted towards shorter wavelengths. The absorbance of the medium is then read at 570 nm (absorption peak of resorufin) and at 600 nm (absorption peak of resazurin) in a microplate reader (BioTek ELx800). The absorbance measured at 570 nm is subtracted by the value measured at 600 nm and by the value corresponding to the absorption of the medium only control. The result is proportional to the number of cells and is presented as (value ± standard combined uncertainty). Before and after each test, cells on control wells are inspected under an inverted microscope to assure normal development and sterile conditions.

To assess the morphology of cells seeded on both types of scaffolds, cells were fixed with glutaraldehyde 48 h after seeding and observed with a scanning electron microscope (Zeiss DSM 962).

RESULTS AND DISCUSSION

Solution Properties

The nature of the polymer (or polymer blend) and solvent (or solvents) used and their concentrations determine the viscosity, surface tension, and conductivity of the solution. These properties, which are decisive for the success of the electrospinning process, are summarized in Table I in the case of the six PCL solutions used. The surface tension of the solutions is

Table II. Summary of Results Reported for the Electrospinning of PCL Dissolved in Different Pure Solvents

PCL concentration	Solvent	Spinning conditions	Fiber characteristics	Reference
10 wt %	Chloroform	1.0 mm, 6 ml h^{-1}, 13 kV	Average diameter (400 ± 200) nm	12
5–7 wt %	Chloroform	20G, 6 ml h^{-1}, 25–40 kV, 7.5 cm	Average diameters on the order of 300–900 nm	13
12.5% w/v	Chloroform	0.6 ml h^{-1}, 13 kV, 20 cm	Diameters ranging from 1.5 to 6 μm with a percentage of nanofibrils (600 ± 400) nm diameter	14
9–15 wt %	Chloroform	18 G, 6–15 ml h^{-1}, 20 kV, 19.4 cm	Oval-shaped indentations. Diameters from 300–400 nm up to 6–7 μm	15
12 wt %	Chloroform	21 G, 0.7 ml h^{-1}, 20 kV, 10 cm	Diameters in the range 200–500 nm	16
10–15 wt %	Methylene chloride	1.0 mm, 3–50 kV	Average diameter was 5.5 μm for the 13% solution	21
11 wt %	Methylene chloride	1.84 ml h^{-1}, 15 kV, 15 cm	Average diameter (4 ± 2) μm	22
3–10% w/v	Hexafluoropropanol	18 G, 3 ml h^{-1}, 20 kV, 10 cm	5% solution yielded fibers with average diameters ranging from 570 to 1350 nm	23
20 wt %	Acetic acid	0.5 ml h^{-1}, 15 kV, 20 cm	Fiber diameter in the interval 1–2 μm	27
20 wt %	Acetic acid	22 G, 0.3 ml h^{-1}, 6 kV, 10 cm	Average diameter (1.36 ± 0.33) μm	This work
8 wt %	Chloroform	23 G, 0.6 ml h^{-1}, 13 kV, 28 cm	Average diameter (3.10 ± 0.45) μm	This work

Spinning conditions listed are (when reported): needle gauge or internal diameter, feed rate, high voltage, and needle-collector distance.

slightly above the surface tension of the solvents which are tabulated as 27.1 mN m^{-1} for acetic acid and 26.67 mN m^{-1} for chloroform, both at 25°C.[55] The differences in surface tension among the solutions are small and, therefore, not expected to motivate different behaviors during electrospinning. The conductivity of the solutions is very low and showed a slight tendency to decrease when the polymer concentration increased from 14 to 26 wt %. A low conductivity makes the stretching of the jet during electrospinning less effective due to the small current transported by the jet and consequently reduced repulsion between charges. The addition of PCL decreased the conductivity, when compared with that of acetic acid (0.057 μS cm^{-1}), due to a lower mobility of charge carriers in the presence of the nonconducting polymer. Both surface tension and conductivity values are close to those of the solvent, showing this is predominant in determining those properties. Zero shear viscosity exhibited the strongest variation, increasing sharply with polymer concentration: this will have, as shown below, dramatic consequences on the outcome of the electrospinning process.

Electrospinning Parameters

A preliminary study of the effect of several parameters that influence the outcome of the electrospinning process—polymer concentration, high voltage applied to the polymer source, needle-collector distance, and feed rate—allowed us to determine a set of parameters suitable for successfully electrospinning PCL dissolved in acetic acid. The lowest polymer concentration required was 20 wt % and the standard electrospinning process parameters were the following: high voltage, 6.0 kV; needle-collector distance, 10 cm; feed rate, 0.3 mL h^{-1}. Other sets of parameters might also yield good quality fibers: we opted for using these because they correspond to the lowest polymer concentration and lowest voltage found to be adequate for the production of fibers from a precursor solution of PCL dissolved in acetic acid.

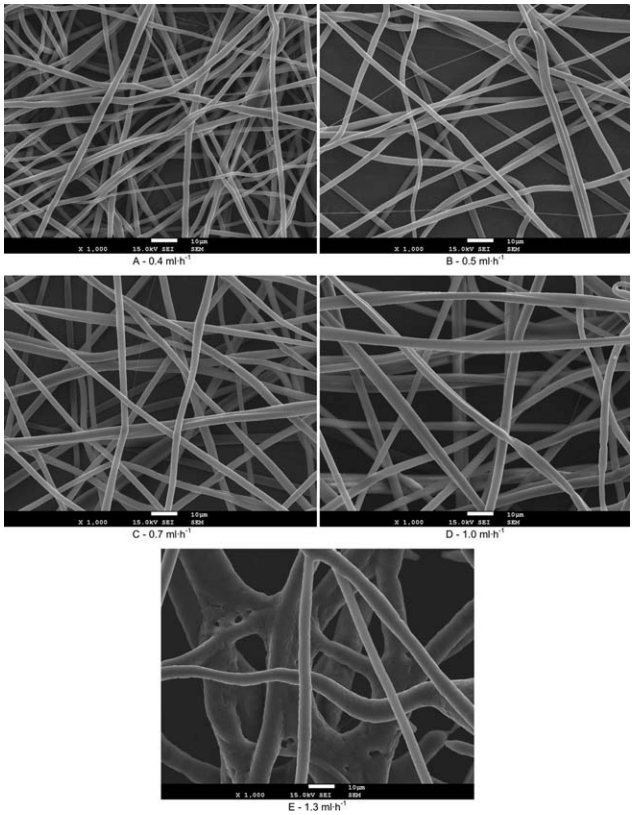

Figure 2. Effect of the solution feed rate on the morphology of the fibers obtained with the solution of 20 wt % PCL in acetic acid.

Table III. Average Fiber Diameter of PCL Mats Obtained with Different Solvents and Feed Rates

Mat reference	PCL concentration (wt %)	Solvent	Feed rate Φ/(ml h^{-1})	Average fiber diameter (μm)
Aa03	20	Acetic acid	0.3	1.36 ± 0.33
Aa04			0.4	1.96 ± 0.52
Aa05			0.5	2.35 ± 0.41
Aa07			0.7	2.74 ± 0.44
Aa10			1.0	3.36 ± 0.58
Ch06	8	Chloroform	0.6	3.10 ± 0.45

Effect of PCL Concentration

The morphology of the fibers changed dramatically with PCL concentration. Increasing the PCL concentration from 14 to 26 wt % also increased the zero shear viscosity of the solutions from 4.4 to 81 Pa s. The viscosity of the solutions has a strong influence on the outcome of the spinning process. A low viscosity eases the stretching of the fibers, but, as can be seen in Figure 1(A,B), the production of thinner fibers from the less viscous 14 and 17 wt % PCL solutions is accompanied by the formation of large beads. These beads are formed when the forces associated with the surface tension are strong enough to cause a displacement of the solution along the jet to yield local minima of surface to volume ratio. The fibers obtained from the 20 and 23 wt % PCL solutions are of good quality [Figure 1(C,D)], with average diameters of (1.36 ± 0.33) μm and (1.71 ± 0.30) μm, respectively. The solution with a 26 wt % concentration of PCL originated mostly large, fused, and poor quality fibers, as a consequence of the incomplete evaporation of the solvent and of high viscoelastic forces resisting the stretching of the jet [Figure 1(E)]. The fibers obtained when chloroform was used as solvent are illustrated in Figure 1(F). Even when using the lowest concentration (8 wt %) and flow rate (0.6 mL h^{-1}), with which we managed to have a stable process, the average diameter of the fibers is (3.10 ± 0.45) μm, more than the double of that obtained using acetic acid as a solvent and the 20 wt % solution. This is a clear consequence of the higher volatility of chloroform and of the lower conductivity of this solution.

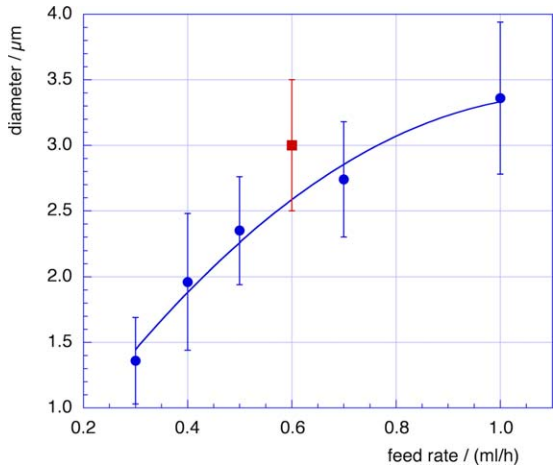

Figure 3. Plot of PCL fiber diameter as function of solution feed rate. Vertical bars represent the interval [average ± experimental standard deviation]. Circles: 20 wt % PCL dissolved in acetic acid; square: 8 wt % PCL dissolved in chloroform. [Color figure can be viewed in the online issue, which is available at wileyonlinelibrary.com.]

Table II presents a summary of the main results reported in the literature for the electrospinning of PCL dissolved in different pure solvents. When compared to our results, we see that the successful electrospinning of PCL dissolved in acetic acid requires much higher concentrations and the use of much smaller voltages. The resulting fibers are in the upper range of diameters obtained by other authors.

Solution Feed Rate

Varying the solution feed rate is an effective way of achieving fibers with different average diameters.[44] The amount of polymer solution reaching the needle tip and, therefore, available to be extracted by the force exerted by the electric field on the charged solution varies in accordance with any increase or decrease of the feed rate. The range of useable feed rates is limited by two factors: a small feed rate may lead to interruptions in the jet due to the unavailability of sufficient solution and a high feed rate may lead to an accumulation of solution at the needle tip due to an insufficient extraction rate. The effect of varying the feed rate from 0.3 mL h^{-1} up to 1.3 mL h^{-1} can be seen in Figure 1(C) (for the 0.3 mL h^{-1} rate) and Figure 2 (for the rates 0.4–1.3 mL h^{-1}). The fibers are of good quality up to 1.0 mL h^{-1}. For the highest feed rate most fibers are ill formed. The diameters of the fibers are listed in Table III and plotted in Figure 3. The fiber diameters increase with feed rate but at a pace that decreases with increasing feed rate. The average fiber diameter obtained using chloroform as a solvent is only slightly higher than when acetic acid was used (for the same feed rate),

Table IV. Apparent Density, Porosity, and Elastic Modulus of PCL Fiber Mats at Different Solution Feed Rates

Fiber mat	Apparent density $\rho_{apparent}$/(g cm^{-3})	Porosity P (%)	Young's modulus Y /(10^6 Pa)
Aa03	0.20 ± 0.02	83 ± 2	6.6 ± 1.1
Aa05	0.20 ± 0.01	82 ± 1	6.8 ± 0.8
Aa07	0.21 ± 0.01	82 ± 1	7.1 ± 0.9
Aa10	0.22 ± 0.02	81 ± 2	7.6 ± 0.9
Ch06	0.20 ± 0.02	82 ± 2	4.7 ± 0.9

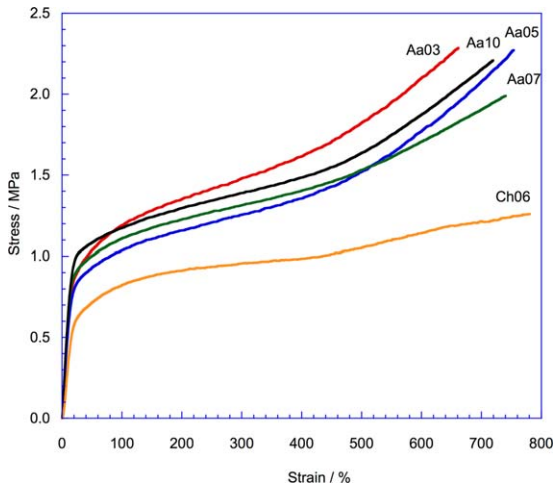

Figure 4. Typical stress–strain curves for PCL fiber mats electrospun from the 20 wt % in acetic acid solution at four different feed rates and from the 8 wt % in chloroform solution. [Color figure can be viewed in the online issue, which is available at wileyonlinelibrary.com.]

but it should be noted that this is achieved using a concentration, which is only 40% of that used with acetic acid. Table III also defines a reference by which all mats will be referenced to hereafter.

Fiber Mat Porosity

The porosity of the PCL fiber mats, evaluated from the apparent density, is shown in Table IV. All mats exhibit a high porosity, slightly above 80%, which is typical of electrospun nonwoven mats and a requirement of a scaffold for tissue engineering applications.[41,56] This porosity is a consequence of the shape and arrangement of the fibers and independent of their diameter.

Mechanical Properties

Tensile tests of mats produced from the 20 wt % PCL in acetic acid solution using four different feed rates were performed in order to determine if any correlation between fiber diameter and mechanical properties exists. Mats obtained from the 8 wt % PCL in chloroform solution were also tested to compare the mechanical behavior of PCL fiber mats electrospun from solutions prepared using glacial acetic acid or chloroform as solvent. Stress–strain curves of the nanofiber mats are shown in Figure 4. The curves are very similar for all feed rates used, suggesting there is no strong dependence of Young's modulus on PCL fiber diameter, at least in the interval [1.4; 3.4] μm where average fiber diameters lie. The Young's modulus of the PCL fiber mats is shown in Table IV. A slight increase in Young's modulus with PCL fiber diameter is seen, with the differences between Aa03 and Aa10 and between Aa05 and Aa10 being statistically significant ($p < 0.05$). The PCL fiber mats obtained using chloroform as solvent display a smaller Young's modulus than those obtained using acetic acid as solvent. The differences between Ch06 and all Aa mats are statistically significant ($p < 0.001$). All fiber mats sustained strains above 700%, up to the maximum elongation allowed by the equipment.

X-ray Diffraction

The X-ray diffraction spectra of the five PCL fiber mats are shown in Figure 5(A). The spectra are very similar: all of them display two prominent crystalline peaks at 21.5° and 23.9° due to diffraction by the (110) and (200) planes, respectively.[57] Smaller peaks at 15.7°, 22.2°, and 24.5° are due to diffraction by the (102), (111), and (201) planes. Diffraction by the (210) and (211) planes result in two peaks that appear convoluted at 30.0°. Figure 5(B) shows the fitting of the diffractogram of the Aa03 fiber mat by a sum of Voigt functions and a constant background. The resulting fit adjusts itself very well to the diffractogram. From the fittings performed to all diffraction spectra it was possible to calculate the degree of crystallinity of the fibers. The degree of crystallinity of the Aa fibers shows a slight tendency to decrease with fiber diameter. The Ch06 mat exhibits the highest crystallinity: in spite of the faster evaporation and consequent rapid solidification of the jet, chloroform, being a better solvent for PCL, allows a better organization of the PCL molecules. This fact is also evidenced by the bigger size of the crystallites present in the Ch06 fibers. Crystallite size was calculated using the Scherrer equation, FWHM and position of the maximum intensity peak. Results are shown in Table V. The

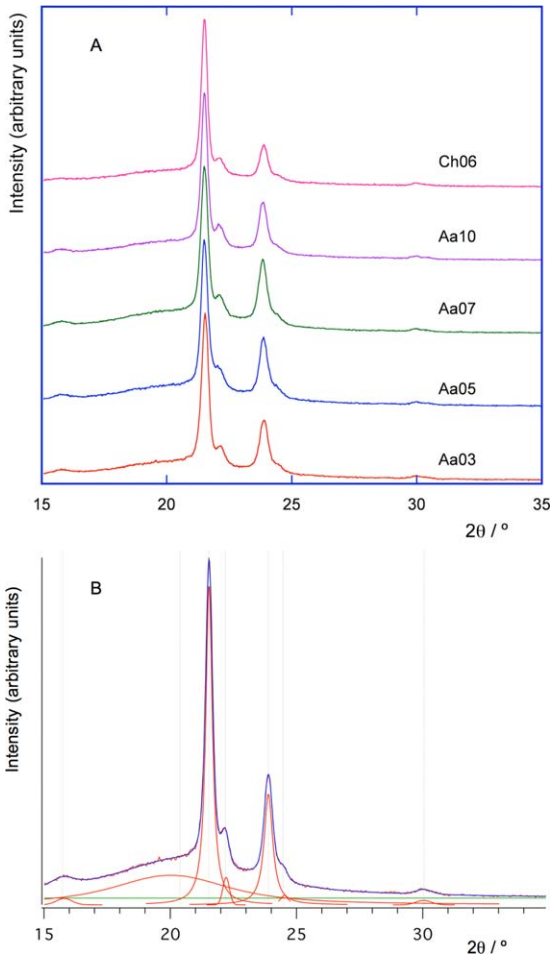

Figure 5. (A) Diffractograms of PCL mats obtained using chloroform and acetic acid as solvents. (B) Fitting of the characteristic peaks of the PCL Aa03 mat diffractogram with Voigt functions and a constant background. The peak located at 20.4° corresponds to the amorphous halo. The remaining peaks arise from crystalline diffractions. [Color figure can be viewed in the online issue, which is available at wileyonlinelibrary.com.]

Table V. X-ray Diffraction Results for Crystallinity and Crystallite Size for the PCL Mats

Fiber mat	Crystallinity $w_{c,x}$ (%)	FWHM (°)	Crystallite size t_c (nm)
Aa03	37.7 ± 0.8	0.326	25.9
Aa05	36.9 ± 1.0	0.311	27.1
Aa07	35.6 ± 0.6	0.334	25.3
Aa10	35.3 ± 0.7	0.294	28.7
Ch06	40.6 ± 1.9	0.267	31.6

Ch06 mats exhibit the highest degree of crystallinity and crystallite size. (FWHM—Full width at half maximum). All PCL fiber mats exhibit the same apparent density and porosity. Ch06 mats have the lowest elastic modulus, with the differences between the Ch06 mat and all Aa mats being statistically significant ($p < 0.001$).

higher crystallinity and crystallite size of Ch06 fibers is in apparent contradiction with the lower Young's modulus of these fiber mats. However, the crystalline regions of the fibers may be acting like a nonreinforcing filler in a composite, with the amorphous phase being more easily deformed by the tensile stress applied. Another explanation lies in the structure of the nonwoven mat. Whereas XRD probes the structure of the individual fibers, tensile tests probe the properties of the whole nonwoven mat where the interaction of the individual fibers is also of importance. Residual acetic acid may cause some crosslinking of the fibers leading to an increased elastic modulus. Since chloroform evaporates faster, less solvent is still present in the fibers when they reach the collector and the reinforcing effect of interfiber crosslinking is smaller.

Cell Adhesion and Proliferation

To analyze cell adhesion and proliferation on PCL scaffolds obtained from the different solvents we chose to use the Ch06 scaffolds, wherein 8% wt PCL was dissolved in chloroform, and produce new membranes of electrospun 20%wt PCL dissolved in acetic acid using a flow rate of 0.8 mL h^{-1}, Aa08, to obtain similar fiber diameters (Figure 3). Moreover, to verify the influence of fiber diameter on the results we choose to use also the Aa03 scaffolds.

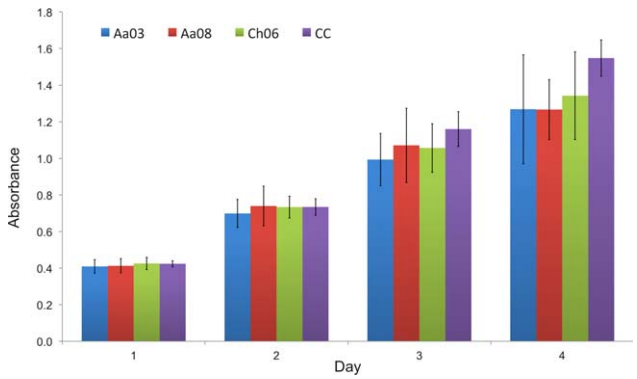

Figure 6. Daily absorbance measurements of resazurin cell viability assay in scaffolds produced with PCL dissolved in acetic acid (Aa03 and Aa08) and in chloroform (Ch06) and on a cell control culture in a 24 well plate (CC). [Color figure can be viewed in the online issue, which is available at wileyonlinelibrary.com.]

As we can observe in Figure 6, on the first day the absorbance values are about the same for all three scaffolds and for the cell control culture (CC). No significant differences between the absorbance results for the scaffolds were observed during the following days of culture. On days three and four the absorbance results in control wells exhibits slightly higher values when compared with the results for the scaffolds. On the fourth day the absorbance results of the three scaffolds are higher than 80% of that of the control cells. These results show that Vero cells adhere and proliferate equally well on both types of scaffold and irrespective of fiber diameter in the interval studied.

Cells fixed with glutaraldehyde 48 h after seeding were observed by SEM (Figure 7). It can be seen that cells attach to the fibers and adopt an extended morphology. There are no apparent differences in the morphology of cells grown on the different scaffolds, even though the average fiber diameter of the Aa03 scaffold is approximately half the average fiber diameter of the other two scaffolds.

Despite the high porosity of the scaffolds, cells are mainly on the scaffolds surface. This is an indication that the pore size is not sufficient to allow cell migration into the structure.

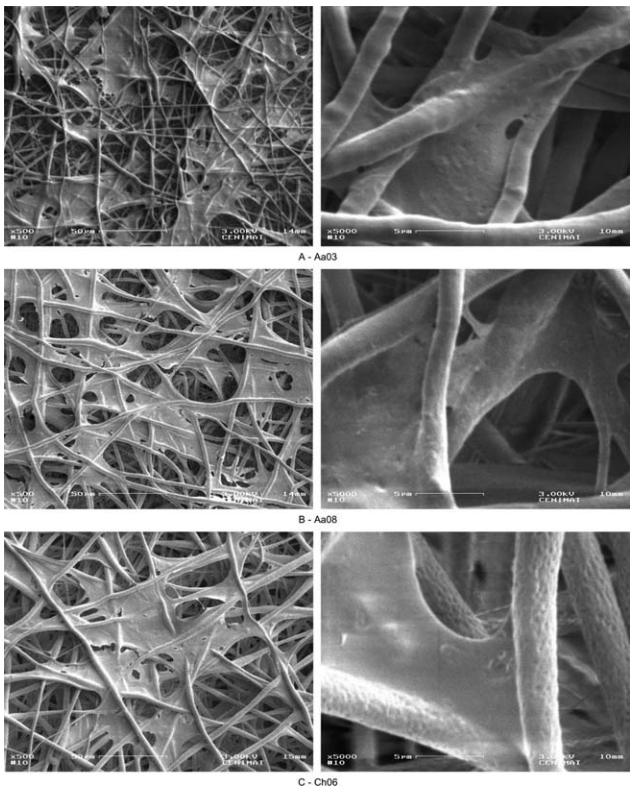

Figure 7. SEM images of Vero cells growing on the three types of PCL scaffolds. Overall view (left column) and high magnification view (right column).

CONCLUSIONS

The production of high quality PCL microfibers with diameters in the few micrometers range by electrospinning PCL dissolved in glacial acetic acid is feasible without the use of helper solvents or additives by simply tuning both solution and processing parameters. We studied the relationship between polymer concentration and fiber morphology and concluded that the 20 and 23 wt % solutions yield regular microfibers for the standard processing parameters used. Lower concentrations yield beaded fibers and higher concentrations are too viscous and yield irregular and fused fibers. Varying the flow rate between 0.3 mL h^{-1} and 1.0 mL h^{-1} caused the average fiber diameter to vary between (1.36 ± 0.33) μm and (3.36 ± 0.58) μm.

The fiber mats thus obtained have a Young's modulus which increased from (6.6 ± 1.1) MPa to (7.6 ± 0.9) MPa as the flow rate increased from 0.3 to 1.0 mL h^{-1}. The fiber mats are semi-crystalline, showing a degree of crystallinity between (35.3 ± 0.7)% and (37.7 ± 0.8)% and crystallite sizes in the range 25–30 nm. The PCL fiber mats obtained using chloroform as a solvent displayed a smaller Young's modulus and higher degree of crystallinity and crystallite sizes, a consequence of the better solubility of PCL in chloroform.

Cell viability assay performed on scaffolds obtained by dissolving PCL in acetic acid and in chloroform show that Vero cells adhesion and proliferation rates on the scaffolds are similar, with no statistically significant differences, and therefore not dependent neither on the solvent used to electrospin PCL nor on the diameter of the resulting fibers.

Electrospinning PCL dissolved in acetic acid, a solvent that can be easily neutralized and washed away from the fibers without leaving toxic residues, as the results show, is an interesting alternative for tissue engineering applications: unlike chloroform, acetic acid is miscible with polar solvents, which may allow easier blending of PCL with hydrophilic polymers and therefore achieve the production of electrospun nanofibers with improved properties.

ACKNOWLEDGMENTS

The authors acknowledge funding from "Fundação para a Ciência e a Tecnologia", Portugal, through the projects PTDC/SAU-BMA/109886/2009 and PEst-OE/FIS/UI0068/2011. S. Gomes acknowledges financial support from "Fundação para a Ciência e a Tecnologia", Portugal, through grant SFRH/BD/37854/2007.

REFERENCES

1. Langer, R.; Vacanti, J. *Science* **1993**, *260*, 920.
2. Atala, A. *J. Tissue Eng. Regener. Med.* **2007**, *1*, 83.
3. Lannutti, J.; Reneker, D.; Ma, T.; Tomasko, D.; Farson, D. *Mater. Sci. Eng. C: Biomimetic. Supramol. Syst.* **2007**, *27*, 504.
4. Smith, L.; Liu, X.; Ma, P. *Soft Matter* **2008**, *4*, 2144.
5. Khil, M.; Bhattarai, S.; Kim, H.; Kim, S.; Lee, K. *J. Biomed. Mater. Res. Part B* **2005**, *72B*, 117.
6. Sarasam, A.; Madihally, S. *Biomaterials* **2005**, *26*, 5500.
7. Thomas, V.; Jagani, S.; Johnson, K.; Jose, M.; Dean, D.; Vohra, Y.; Nyairo, E. *J. Nanosci. Nanotechnol.* **2006**, *6*, 487.
8. Williamson, M.; Black, R.; Kielty, C. *Biomaterials* **2006**, *27*, 3608.
9. Prabhakaran, M.; Venugopal, J.; Chan, C.; Ramakrishna, S. *Nanotechnology* **2008**, *19*, 455102.
10. Reed, C.; Han, L.; Andrady, A.; Caballero, M.; Jack, M.; Collins, J.; Saba, S.; Loboa, E.; Cairns, B.; Aalst, J. *Ann. Plast. Surg.* **2009**, *62*, 505.
11. Tillman, B.; Yazdani, S.; Lee, S.; Geary, R.; Atala, A.; Yoo, J. *Biomaterials* **2009**, *30*, 583.
12. Yoshimoto, H.; Shin, Y.; Terai, H.; Vacanti, J. *Biomaterials* **2003**, *24*, 2077.
13. Hsu, C.; Shivkumar, S. *J. Mater. Sci.* **2004**, *39*, 3003.
14. Vaz, C.; van Tuijl, S.; Bouten, C.; Baaijens, F. *Acta Biomater.* **2005**, *1*, 575.
15. Buschle-Diller, G.; Cooper, J.; Xie, Z.; Wu, Y.; Waldrup, J.; Ren, X. *Cellulose* **2007**, *14*, 553.
16. Sajeev, U. S.; Anand, K. A.; Menon, D.; Nair, S. *Bull. Mater. Sci.* **2008**, *31*, 343.
17. Reneker, D.; Kataphinan, W.; Theron, A.; Zussman, E.; Yarin, A. *Polymer* **2002**, *43*, 6785.
18. Theron, S.; Zussman, E.; Yarin, A. *Polymer* **2004**, *45*, 2017.
19. Yarin, A.; Kataphinan, W.; Reneker, D. *J. Appl. Phys.* **2005**, *98*, 064501.
20. Wong, S. C.; Baji, A.; Leng, S. *Polymer* **2008**, *49*, 4713.
21. Lee, K.; Kim, H.; Khil, M.; Ra, Y.; Lee, D. *Polymer* **2003**, *44*, 1287.
22. Paneva, D.; Bougard, F.; Manolova, N.; Dubois, P.; Rashkov, I. *Eur. Polym. J.* **2008**, *44*, 563.
23. Lee, S. J.; Oh, S. H.; Liu, J.; Soker, S.; Atala, A.; Yoo, J. *J. Biomaterials* **2008**, *29*, 1422.
24. Kim, G. H. *Biomed. Mater.* **2008**, *3*, 025010.
25. Moghe, K.; Hufenus, R.; Hudson, S. M.; Gupta, B. S. *Polymer* **2009**, *50*, 3311.
26. Schueren, L. V.; Schoenmaker, D.; Kalaoglu, O. I.; Clerck, K. *Eur. Polym. J.* **2011**, *47*, 1256.
27. Kanani, A. G.; Bahrami, S. H. *J. Nanomater.* **2011**, *2011*, 724153.
28. Sinha, V.; Bansal, K.; Kaushik, R.; Kumria, R.; Trehan, A. *Int. J. Pharm.* **2004**, *278*, 1.
29. Ohkawa, K.; Kim, H.; Lee, K. *J. Polym. Environ.* **2004**, *12*, 211.
30. Tan, E.; Ng, S.; Lim, C. *Biomaterials* **2005**, *26*, 1453.
31. Ghasemi-Mobarakeh, L.; Morshed, M.; Karbalaie, K.; Fesharaki, M.; Nasr-Esfahani, M. H.; Baharvand, H. *Yakhteh Med. J.* **2008**, *10*, 179.
32. Sun, L.; Han, R. P. S.; Wang, J.; Lim, C. T. *Nanotechnology* **2008**, *19*, 455706.
33. Fridrikh, S.; Yu, J.; Brenner, M.; Rutledge, G. *Phys. Rev. Lett.* **2003**, *90*, 144502.
34. Chen, F.; Lee, C. N.; Teoh, S. H. *Mater. Sci. Eng. C: Biomimetic Supramol. Syst.* **2007**, *27*, 325.

35. Venugopal, J. R.; Low, S.; Choon, A. T.; Kumar, A. B.; Ramakrishna, S. *Artif. Organs* **2008**, *32*, 388.
36. Prabhakaran, M. P.; Venugopal, J. R.; Chyan, T. T.; Hai, L. B.; Chan, C. K.; Lim, A. Y.; Ramakrishna, S. *Tissue Eng. Part A* **2008**, *14*, 1787.
37. Zhang, Y.; Ouyang, H.; Lim, C.; Ramakrishna, S.; Huang, Z. *J. Biomed. Mater. Res. Part B* **2005**, *72B*, 156.
38. Venugopal, J.; Zhang, Y.; Ramakrishna, S. *Nanotechnology* **2005**, *16*, 2138.
39. Panseri, S.; Cunha, C.; Lowery, J.; Del Carro, U.; Taraballi, F.; Amadio, S.; Vescovi, A.; Gelain, F. *Biotechnology* **2008**, 8.
40. Ramakrishna, S.; Fujihara, K.; Teo, W.-E.; Ma, Z. In An introduction to Electrospinning and Nanofibers; World Scientific, Singapore **2005**.
41. Greiner, A.; Wendorff, J. H. *Angew. Chem. Int. Ed. Engl.* **2007**, *46*, 5670.
42. Schiffman, J. D.; Schauer, C. L. *Polym. Rev.* **2008**, *48*, 317.
43. Reneker, D. H.; Yarin, A. L. *Polymer* **2008**, *49*, 2387.
44. Henriques, C.; Vidinha, R.; Botequim, D.; Borges, J. P.; Silva J. A. M. C. *J. Nanosci. Nanotechnol.* **2009**, *9*, 3535.
45. Canejo, J. P.; Borges, J. P.; Godinho, M. H.; Brogueira, P.; Teixeira, P. I. C.; Terentjev, E. M. *Adv. Mater.* **2008**, *20*, 4821.
46. Franco, P. Q.; João, C. F. C.; Silva, J. C.; Borges, J. P. *Mater. Lett.* **2012**, *67*, 233.
47. Teo, W. E.; Ramakrishna, S. *Nanotechnology* **2006**, *17*, R89.
48. Moghe, A. K.; Gupta, B. S. *Polym. Rev.* **2008**, *48*, 353.
49. Yu, D. G.; Yu, J. H.; Chen, L.; Williams, G. R.; Wang, X. *Carbohydr. Polym.* **2012**, *90*, 1016.
50. Yu, D. G.; Chian, W.; Wang, X.; Li, X. Y.; Li, Y.; Liao, Y. Z. *J. Memb. Sci.* **2013**, *428*, 150.
51. Crespy, D.; Friedmann, K.; Popa, A. *Macromol. Rapid Commun.* **2012**, *33*, 1978.
52. Townsend-Nicholson, A.; Jayasinghe, S. N. *Biomacromolecules* **2006**, *7*, 3364.
53. Gaumer, J.; Prasad, A.; Lee, D.; Lannutti, J. *Acta Biomater.* **2009**, *5*, 1552.
54. Cullity, B. D.; Stock, S. R. In Elements of X-Ray diffraction, 3rd ed. Prentice-Hall: New Jersey, **2001**.
55. Lide, D. R., Ed. In CRC Handbook of Chemistry and Physics, 89th ed.; CRC Press LLC: Boca Raton, FL, 2009, pp 6–127.
56. Ingavle, G.C.; Leach, J. K. *Tissue Eng. Part B: Rev.* **2014**, DOI: 10.1089/ten.teb.2013.0276.
57. Bittiger, H.; Marchessaul, R. H.; Niegisch W. O. *Acta Crystallogr.* **1970**, *B26*, 1923.